Building Engineering 2023; 1(1): 403.
Original Research Article

Assessing seismic risk in the built environment of Istanbul: High-resolution hazard mapping and ground motion analysis in the sea of Marmara region

Erol Kalkan[1,*], Polat Gülkan[2]

[1] *QuakeLogic Inc., Roseville, CA 95747, USA*

[2] *Baskent University, 06790 Ankara, Turkey*

*** Corresponding author:** Erol Kalkan, erol@quakelogic.net

ARTICLE INFO

Received: 23 October 2023
Accepted: 22 November 2023
Available online: 11 December 2023

doi: 10.59400/be.v1i1.403

ABSTRACT: This research scrutinizes the seismic threat looming over Istanbul, potentially subject to a substantial earthquake. We analyze six plausible earthquake scenarios, utilizing six ground motion prediction equations (GMPEs), to forge high-resolution seismic hazard maps. These maps reveal not only peak horizontal ground accelerations but also spectral acceleration values across varying temporal frames, integrating the amplification effects of softer sediments. Our approach delineates that Istanbul's western shoreline faces heightened risk, with median spectral accelerations at 0.3 s approaching 1 g, signifying intense shaking potential. In contrast, the area encompassing the financial district exhibits lower values, around 0.3 g. The granularity of these findings lays bare the seismic vulnerabilities of the region, offering a window into the risks and potential damages facing this bustling metropolis. This enhanced understanding paves the way for strategic urban planning and risk mitigation efforts aimed at safeguarding Istanbul's populace and infrastructure. This article succinctly condenses our study's pivotal conclusions, presenting a clarion call for proactive measures to diminish earthquake impacts on this dynamic urban landscape.

KEYWORDS: deterministic seismic hazard analysis; Istanbul metropolis; seismic design; site amplification; hazard; earthquake; risk; insurance; sea of Marmara; seismic risks in the building environment; seismic design; seismic-resistant construction

1. Introduction

Istanbul's historical significance is unparalleled, having been the epicenter of several empires, from the Roman to the Ottoman. Its unique geographical positioning along a 30 km strait, which serves as a conduit between the Black Sea and the Sea of Marmara, has long been strategic. Modern-day Istanbul covers an area of 1830 km^2, with its metropolitan expanse reaching 6220 km^2, supporting a dense population of approximately 16 million individuals. However, its illustrious history is marred by a legacy of seismic volatility due to its location within one of Eurasia's most active seismic belts, as evidenced by over ten notable seismic events since 1509, depicted in **Figure 1**.

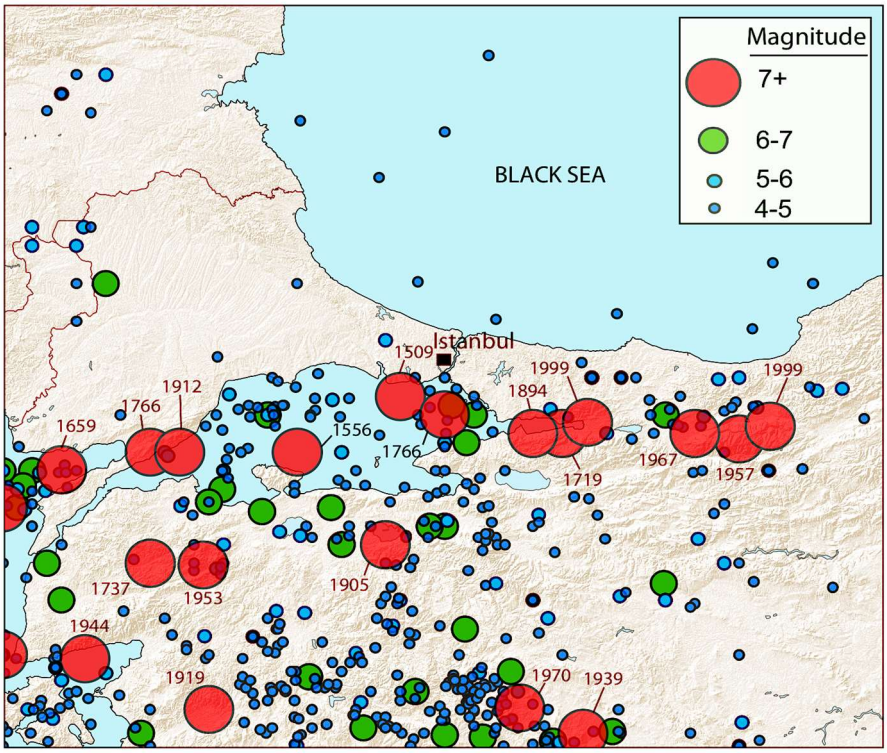

Figure 1. Map of Sea of Marmara (Turkey) region showing historic seismicity. More than ten damaging quakes have occurred since 1509. Within last century, seven earthquakes with M ≥ 7 took place. The earthquake magnitudes are indicated by the size of the circles.

The region's seismicity, particularly illuminated by the 1999 Kocaeli (M7.4) and Düzce (M7.2) earthquakes along the North Anatolian Fault Zone (NAFZ), has had a profound impact on the city's seismic risk profile, as documented in **Figure 2**. The NAFZ, a prominent strike-slip fault system, facilitates right-lateral slip movement between the Anatolian and Eurasian plates and has been characterized by a sequence of significant earthquakes, with magnitudes exceeding 6.7 (**Figure 3**).

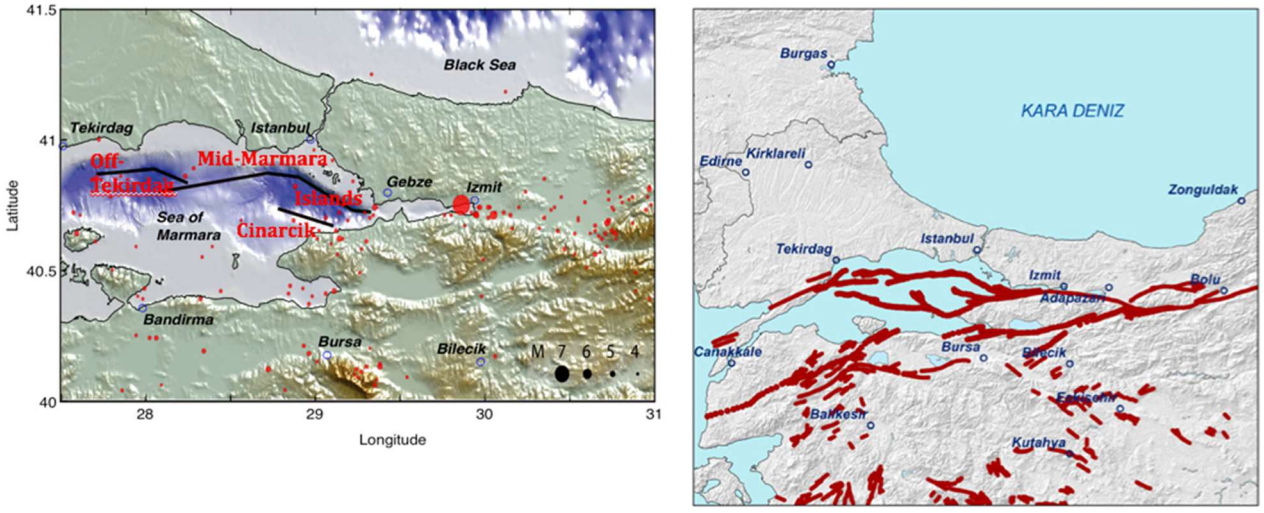

Figure 2. Map of Sea of Marmara (Turkey) region showing instrumental seismicity for the time period 1973–2010. The earthquake magnitudes are indicated by the size of the circles. Also shown are the submarine fault segments (Off-Tekirdağ, Mid-Marmara, Islands, and Çınarcık) under the Sea of Marmara floor; these fault segments may nucleate an M ≥ 6.9 event that may strongly shake the Istanbul Metropolitan Area. Nearest fault segments lie within 10 to 15 km offshore from the city's southern coastline.

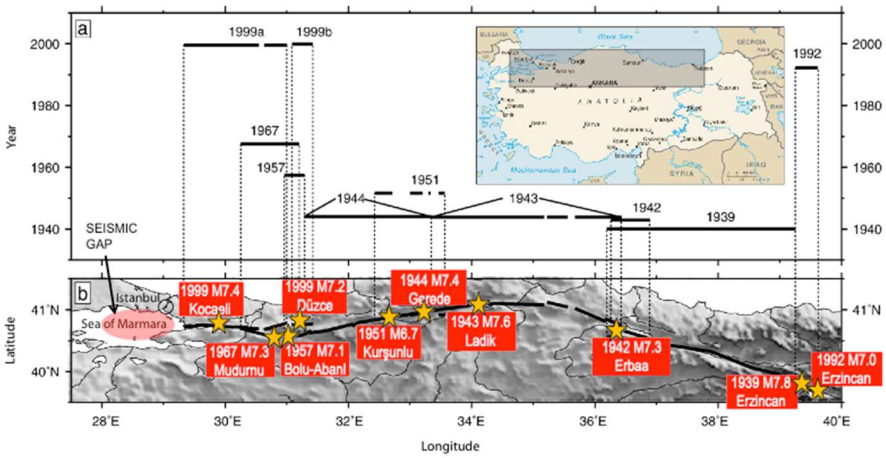

Figure 3. Sequence of westerly propagating ten large (M ≥ 6.7) earthquakes on the North Anatolian Fault Zone (NAFZ), shown with thick black line. Potential seismic gap in the Sea of Marmara is highlighted; also shown are the fault rupture length for each event along the NAFZ; the most recent events of this sequence are the 1999 M7.4 Kocaeli (Izmit) and M7.2 Duzce earthquakes.

This study addresses the critical need for a detailed seismic hazard and risk assessment for Istanbul tailored for earthquake engineering applications. The western extension of the NAFZ, particularly the submarine fault system comprising the Islands, Çınarcık, Mid-Marmara, and Off-Tekirdağ fault segments, poses a pronounced seismic threat to the Istanbul metropolitan area. These segments harbor the potential to generate earthquakes with magnitudes of 7 or greater, which could inflict considerable damage upon the city's infrastructure.

The seismic vulnerability of Istanbul is further exacerbated by its dense population, extensive infrastructure, and the prevalence of high-rise structures. The metropolis hosts numerous essential services, including healthcare, education, and transportation systems, and stands as a pivotal economic center with myriad commercial and industrial operations. Notably, the earthquake exposure concentrated around the Marmara Sea region constitutes 58% of the total regional exposure, with commercial enterprises being the most affected sector, as illustrated in **Figure 4**.

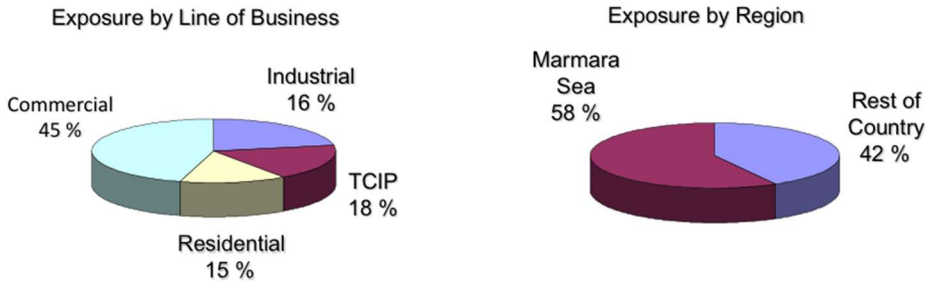

Figure 4. The majority of earthquake exposure, which accounts for 58% of the total, is located around the Marmara Sea region. The largest portion of this exposure is related to commercial lines (Credit: Risk Management Solutions Inc., Newmark, CA).

In light of these findings, the imperative to devise and implement comprehensive seismic risk mitigation strategies for Istanbul cannot be overstated. This research endeavors to fill the existing gap by providing high-fidelity seismic hazard maps and risk assessments, enabling the development of informed engineering solutions and urban planning strategies. By doing so, we aim to enhance the seismic resilience of the Istanbul metropolitan area, ensuring the protection of its inhabitants, the continuity of critical services, and the preservation of its economic vitality in the face of potential seismic catastrophes.

Our work is not only academic in nature but also a foundational piece aimed at guiding the revision of building codes, informing strategic development, and influencing policy-making towards a seismically resilient urban future. It is anticipated that the application of our research findings will lead to a tangible decrease in potential earthquake-induced casualties and property loss, thereby safeguarding the heritage and future prosperity of this historic urban hub.

2. Objective

Seismic hazard assessment is conducted through both probabilistic and deterministic methodologies. Probabilistic Seismic Hazard Analysis (PSHA), which generates maps and related products, plays a critical role in risk evaluation for building codes, earthquake insurance, and the seismic design of essential infrastructure. Prior PSHA endeavors for the Sea of Marmara region, which encompasses Istanbul, were reliant on general descriptions of submarine faults and ground motion prediction equations (GMPEs) from the 1990s. In a pivotal update, Kalkan et al.[1] revisited the region's seismic hazards using a probabilistic approach, adopting the methodology established for the U.S. national seismic hazards maps, with a specific focus on California. These modernized PSHA maps drew from then-available global and local GMPEs and incorporated data on regional faults and both historical and instrumental seismicity.

Conversely, deterministic seismic hazard analysis, often referred to as the 'scenario' method, offers a straightforward and traceable strategy for seismic hazard computation. This approach involves estimating ground motions from a selected subset of potential earthquakes, occasionally representing a single seismic event. For the Sea of Marmara, prior research utilized hybrid simulations to predict peak ground motion values. In this current study, we adopt a deterministic method, employing a range of six local and global GMPEs in a combinatorial manner to address epistemic uncertainty. We've delineated six earthquake scenarios for this task, encompassing single and multiple ruptures on the Islands, Mid-Marmara, Çınarcık, and Off-Tekirdağ fault segments along the NAFZ's western stretch beneath the Sea of Marmara.

The GMPEs are objectively weighted based on their precision in predicting the peak ground motions recorded during the 1999 M7.4 Kocaeli earthquake on the Izmit segment of the NAFZ, just east of Istanbul province. This leads to varied but consistent weights for each GMPE, differing across spectral periods.

The resultant seismic hazard for the region is depicted in high-resolution deterministic hazard maps. These maps, which factor in site effects, detail peak horizontal ground acceleration (PGA) and spectral acceleration (SA) at spectral periods of 0.2, 0.3, 0.5, 1, 1.5, 2, 3, and 4 s with 5-percent damping. The spectral periods of 0.2 and 1 s are particularly significant, often employed as key corner periods for the creation of a smooth design spectrum in structural engineering.

3. Seismotectonics of the Marmara region

Seismic reflection surveys, as explored by Smith et al.[2] and Parke et al.[3], have shed light on the intricate and diverse fault system beneath the Sea of Marmara, extending west from the North Anatolian Fault Zone (NAFZ). While the NAFZ is primarily characterized by right-lateral strike-slip faults near the Marmara Sea's eastern conjunction, a shift occurs beneath the sea. Here, the plate boundary transitions into a trans-tensional system, giving rise to a deep basin as noted by Okay et al.[4] (**Figure 1**). This subsea fault system is not merely a single, uninterrupted strike-slip fault but a series of segmented faults, each with significant normal faulting components. Although the geometry of these faults is well-documented up to a depth of 5 km, uncertainties prevail at greater depths. For this analysis, these segments are presumed to have a vertical dip.

Historically, this zone has witnessed a sequence of powerful earthquakes that have sequentially ruptured along the NAFZ. Notably, the Kocaeli and Düzce earthquakes continued a westward earthquake progression that was initiated with the M7.9 Erzincan earthquake in 1939 along this fault (depicted in **Figure 3**). Considering the 1912 event west of the Sea of Marmara as detailed by Kalkan et al.[1] a seismic gap emerges that has remained inactive for over two centuries (highlighted in **Figure 3**). This gap, spanning roughly 150–160 km, harbors the potential to unleash an earthquake exceeding magnitude 7, as indicated by Hubert-Ferrari et al.[5]. Post-1999 Kocaeli earthquake analyses, such as those by Parsons[6] and Parsons et al.[7], suggest increased shear stress on these fault segments, hinting at their heightened rupture potential.

The region's seismic hazard assessment is complicated by the complexity and variability of the fault system, particularly the vertically dipping segments poised to influence the seismic gap's rupture potential beneath the Sea of Marmara. Recognizing the imminent risk of a significant earthquake, a comprehensive grasp of the fault geometry and rupture dynamics is paramount for a more accurate seismic hazard evaluation.

4. Incorporating site effects for improved seismic hazard assessment

For enhanced precision in ground motion predictions across Istanbul's metropolitan regions, it's crucial to factor in the spatial variation of Vs30 values and their corresponding site effects[8]. Illustrated in **Figure 5** is the Vs30 proxy map, developed following the methodology of Wald and Allen[9], which involves computing topographic slope from a 1-km grid dataset. This map reveals that Vs30 values, indicative of stiff soil to hard rock, span from 400 to 760 m/s along the Sea of Marmara's southern coastline. In contrast, the northern coastlines, abutting the metropolitan areas, exhibit Vs30 values ranging from 200 to 400 m/s.

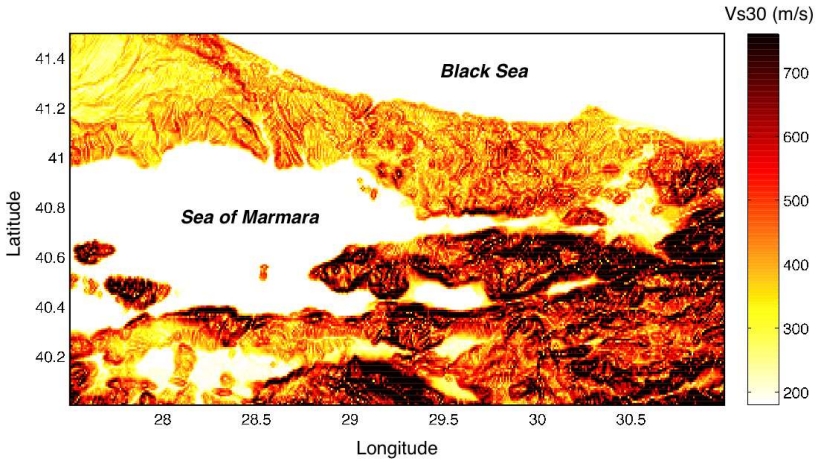

Figure 5. Map of Sea of Marmara (Turkey) region showing a proxy for the shear-wave velocity averaged over the top 30 m of the ground (Vs30) derived from the topographic slope. Dark color = rock site, light color = soft soil site, white color = water. Most of the population in the Istanbul metropolitan area resides on soft-soil deposits, prone to amplified ground shaking during earthquakes (Vs30 data was taken from the USGS).

Particularly noteworthy are the soft sediments, characterized by Vs30 values below 300 m/s, located in the southwestern locales of Istanbul's European side. These areas are more prone to significant ground-shaking amplifications, potentially up to 2.5 times greater than those experienced on the hard rock sites. Therefore, incorporating the spatial variability of Vs30 is indispensable for accurate ground motion estimations pertinent to each specific site within the Istanbul metropolitan expanse.

5. Earthquake scenarios

In the seismic evaluation of the greater Istanbul metropolitan area, our analysis delineated six earthquake scenarios based on potential singular and combined ruptures of the Islands, Mid-Marmara, Çınarcık, and Off-Tekirdağ fault segments. These hypothetical situations, as depicted in **Figure 6**, were informed by historical seismic data and the empirical relationships established by Wells and Coppersmith[10], detailing rupture lengths and anticipated maximum magnitudes (Mmax). For these scenarios, the fault segments in question are presumed to experience strike-slip faulting to their full extent. It is important to note that the earthquakes' hypocenter locations were not considered as variables; the Ground Motion Prediction Equations (GMPEs) employed in this study use specific definitions of distance, such as the closest distance to the co-seismic rupture plane (Rrup) or the closest distance to the surface projection of the causative fault (Rjb). These measures of distance are reliant on the fault's geometry rather than the hypocenter's position.

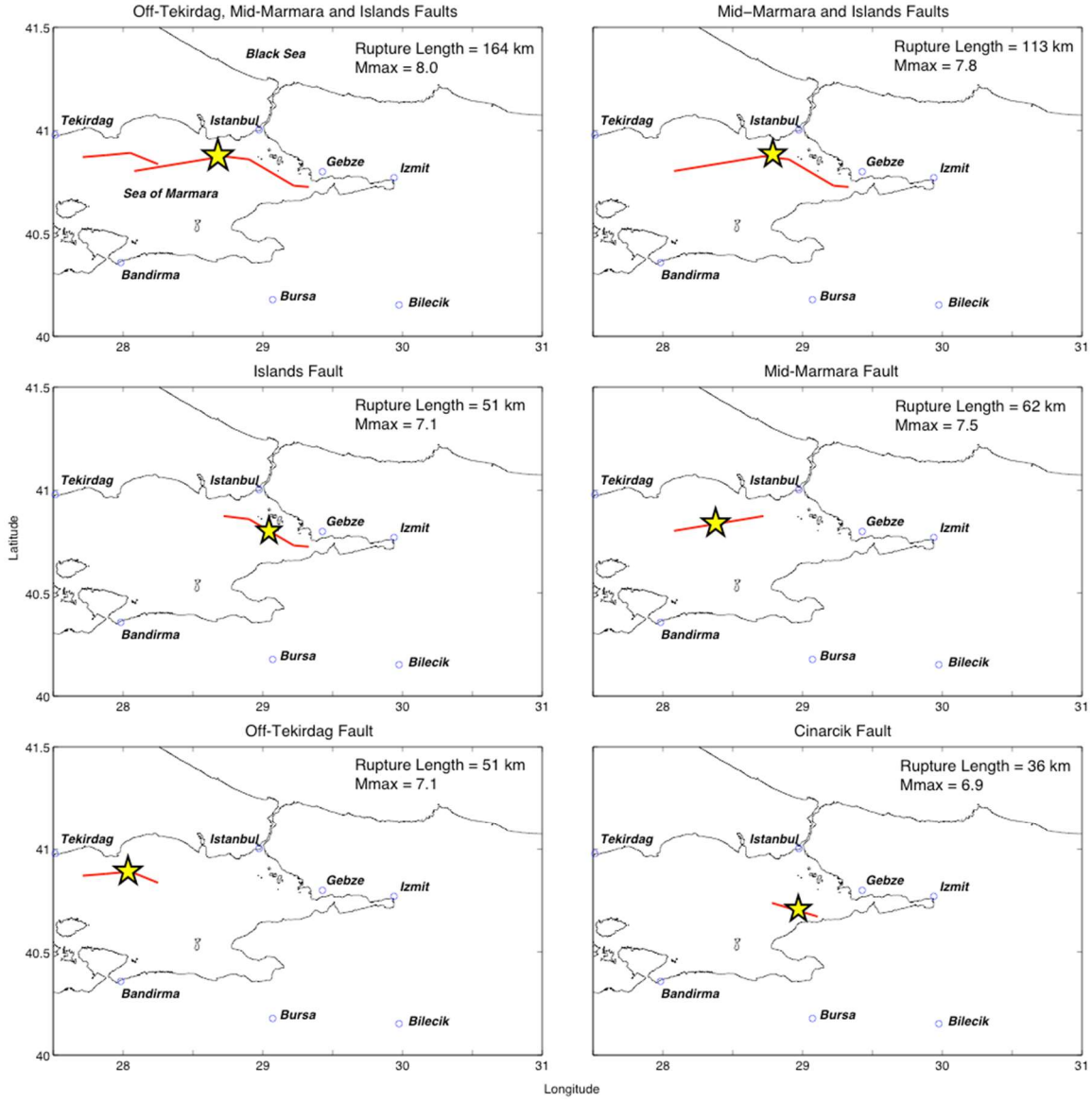

Figure 6. Six earthquake scenarios were defined for the greater Istanbul metropolitan area considering the individual and multiple rupturing of the Islands, Mid-Marmara, Çınarcık and Off-Tekirdağ fault segments. For each scenario, rupture length and expected magnitudes (Mmax) computed according to the historic seismicity and Wells and Coppersmith's[10] empirical equation are shown.

The scenarios outlined herein represent the most significant seismic events that could impact Istanbul, drawn from the understanding that the North Anatolian Fault Zone (NAFZ) is a continuous structure below the Sea of Marmara, as supported by Okay et al.[4] Armijo et al.[11,12], and Le Pichon et al.[13,14]. This continuity suggests that there are no substantial fault offsets that would impede a rupture's progression. While the considerable bends between the Islands and Mid-Marmara, as well as between the Mid-Marmara and Off-Tekirdağ, might theoretically arrest a fault rupture, dynamic faulting models and empirical evidence, such as from the Kocaeli earthquake, indicate that significant fault bends do not invariably halt fault ruptures[15–18]. This understanding is fundamental in recognizing the potential for widespread rupture and its implications for Istanbul's seismic risk assessment.

6. General methodology for hazard computation

The Deterministic Seismic Hazard Analysis (DSHA) methodology is employed to leverage geological and seismic data for identifying potential earthquake sources and calculating the largest conceivable earthquake that each source might generate, given current or theorized tectonic conditions. This hypothetical maximum quake, termed the Maximum Credible Earthquake (MCE), is projected to induce the most significant impact at a specified location. The determination of the MCE incorporates historical seismic records and utilizes the empirical relationship established by Wells and Coppersmith[10], which correlates fault lengths with earthquake magnitudes. By harnessing this data alongside a selection of suitable Ground Motion Prediction Equations (GMPEs) arranged in a logical tree framework, we can derive estimates for Peak Ground Acceleration (PGA) and Spectral Acceleration (SA) across various spectral periods, including 0.2, 0.3, 0.5, 1, 1.5, 2, 3, and 4 s.

6.1. Ground-motion estimation

In our study to quantify seismic hazards while accounting for epistemic uncertainty, we incorporated a suite of six ground-motion prediction equations (GMPEs), which were a blend of global models and those developed specifically for local conditions. The global GMPEs were carefully chosen from the Next Generation of Attenuation (NGA) project, including contributions by Abrahamson and Silva[19], Boore and Atkinson[20], Campbell and Bozorgnia[21], and Chiou and Youngs[22], all of which have been validated for their applicability in Europe and the Middle East, as per the findings of Stafford et al.[23].

Further augmenting our selection, the Graizer and Kalkan[24,25] model, which assimilates data from the NGA project alongside Turkish strong-motion records, was also employed. This model, according to Akkar et al.[26], has demonstrated its efficacy in estimating local ground motions with a precision comparable to its NGA counterparts. For ease of reference within our analysis, the global GMPEs are denoted as AS08, BA08, CB08, CY08, and GK07, respectively. Additionally, the GMPE founded on local data by Kalkan and Gülkan[27] is referred to as KG04.

6.2. Logic tree weighting

To address epistemic uncertainty in hazard analysis, a logic tree approach was utilized. Rather than relying on the subjective weighting of the GMPEs, their expressions were weighted based on the relative accuracy of their performance in predicting peak motions during the 1999 M7.4 Kocaeli earthquake when it ruptured the İzmit segment of the NAFZ up to the eastern reaches of Istanbul, as shown in **Figure 3**. The weighting approach involved assigning a higher weight to a GMPE that demonstrated a smaller overall standard deviation of prediction among other GMPEs. To calculate the relative weights of the GMPEs for each intensity measure (e.g., PGA or spectral accelerations at selected periods), residual analysis was used using the following method:

1) Compute the residuals for the *i*-th GMPE; residuals correspond to the difference between the observations and predictions in natural-log space,
2) Compute the standard deviation of residuals, σ_i for the i^{th} GMPE,
3) Relative weight, W_i, for the *i*-th GMPE is computed as

$$W_i = \left[1/\sigma_i^2\right] / \left[\sum_{i=1,n} \left(1/\sigma_i^2\right)\right]$$

where n is the total number of GMPEs selected and $\sum_{i=1,n}(W_i) = 1$.

Figure 7 illustrates the results of the de-facto segregation showing consistent but varying weights assigned to each GMPE at different spectral periods. Among the six GMPEs, KG04 local GMPE demonstrates the best performance for predicting PGA and spectral acceleration at 0.2, 0.3, 0.5, 1, and 1.5 s, with predictions limited to 2 s. For longer periods (i.e., 3 and 4 s), the remaining five global GMPEs were utilized. AS08 was assigned the highest weight as it has shown superior accuracy in predicting the peak ground motions recorded during the Kocaeli earthquake compared to other GMPEs.

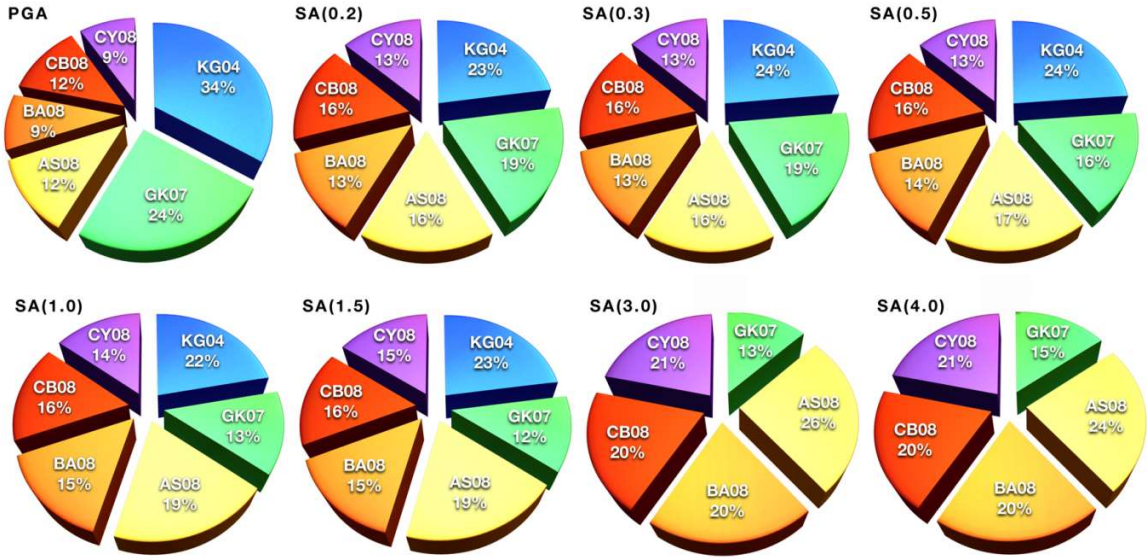

Figure 7. Logic tree weights of GMPEs computed according to their relative performances in predicting the peak motions of the 1994 M7.4 Kocaeli earthquake for PGA and spectral accelerations at 0.2, 0.3, 0.5, 1, 1.5, 2, 3 and 4 s; (local GMPE is KG04[27]; and global GMPEs are GK07[24,25]; AS08[19]; BA08[20]; CB08[21]; CY08[22]).

7. Seismic hazard results

For each earthquake scenario, the following set of maps (with a resolution of 0.002° by 0.002°, or approx. 250 m by 250 m) were generated:

- Median value of peak horizontal ground acceleration (PGA),
- Median value of spectral accelerations (SA) at 0.2, 0.3, 0.5, 1, 1.5, 2, 3, and 4 s for 5%-damping,
- Ratio comparing the shaking level of the 1999 M7.4 Kocaeli event with those in the scenarios for PGA and spectral accelerations,
- Spectral amplification.

Figure 8 displays the median value of PGA for the region for each earthquake scenario, and similarly, **Figures 9** and **10** display the median values of SA at 0.2 and 1.0 sec. These maps incorporate site effects by assigning a Vs30 value corresponding to each grid point by using the map in **Figure 5** as a proxy.

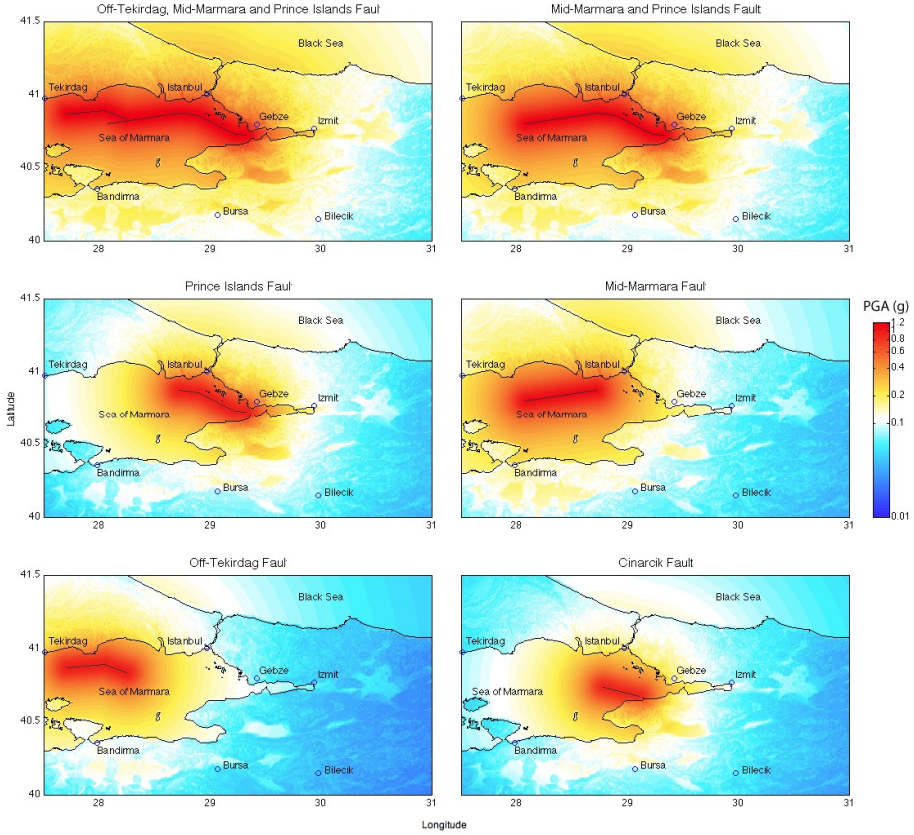

Figure 8. Peak ground acceleration (PGA) estimates for the Sea of Marmara region considering six plausible earthquake scenarios.

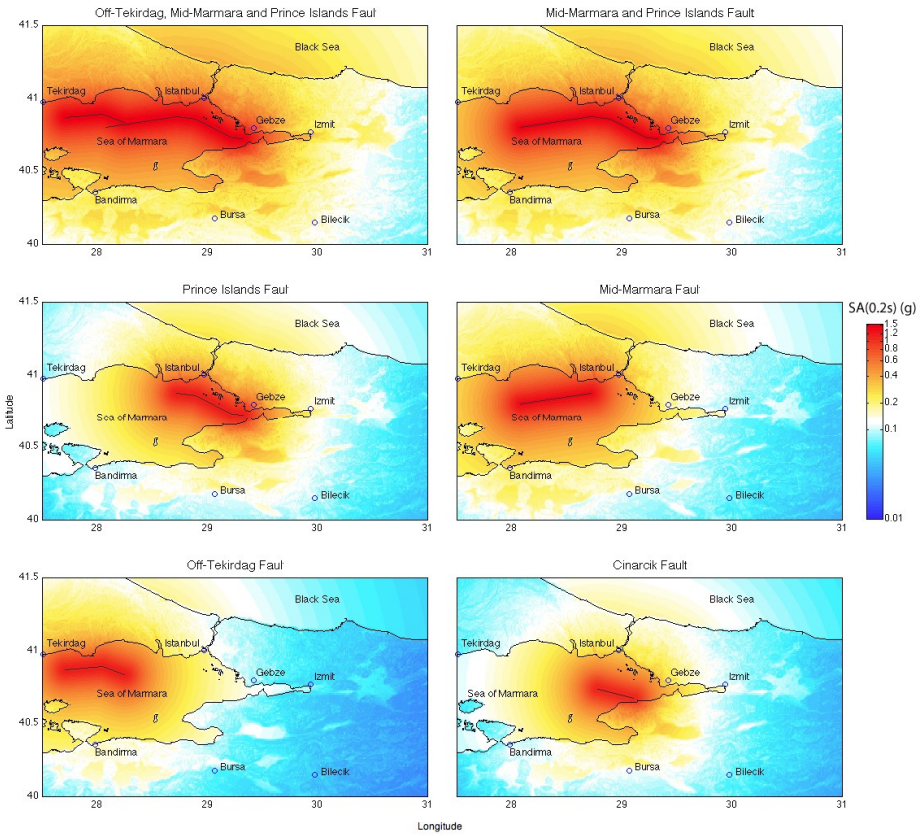

Figure 9. 5%-damped spectral acceleration (SA) at 0.2 sec estimates for the Sea of Marmara region considering six plausible earthquake scenarios.

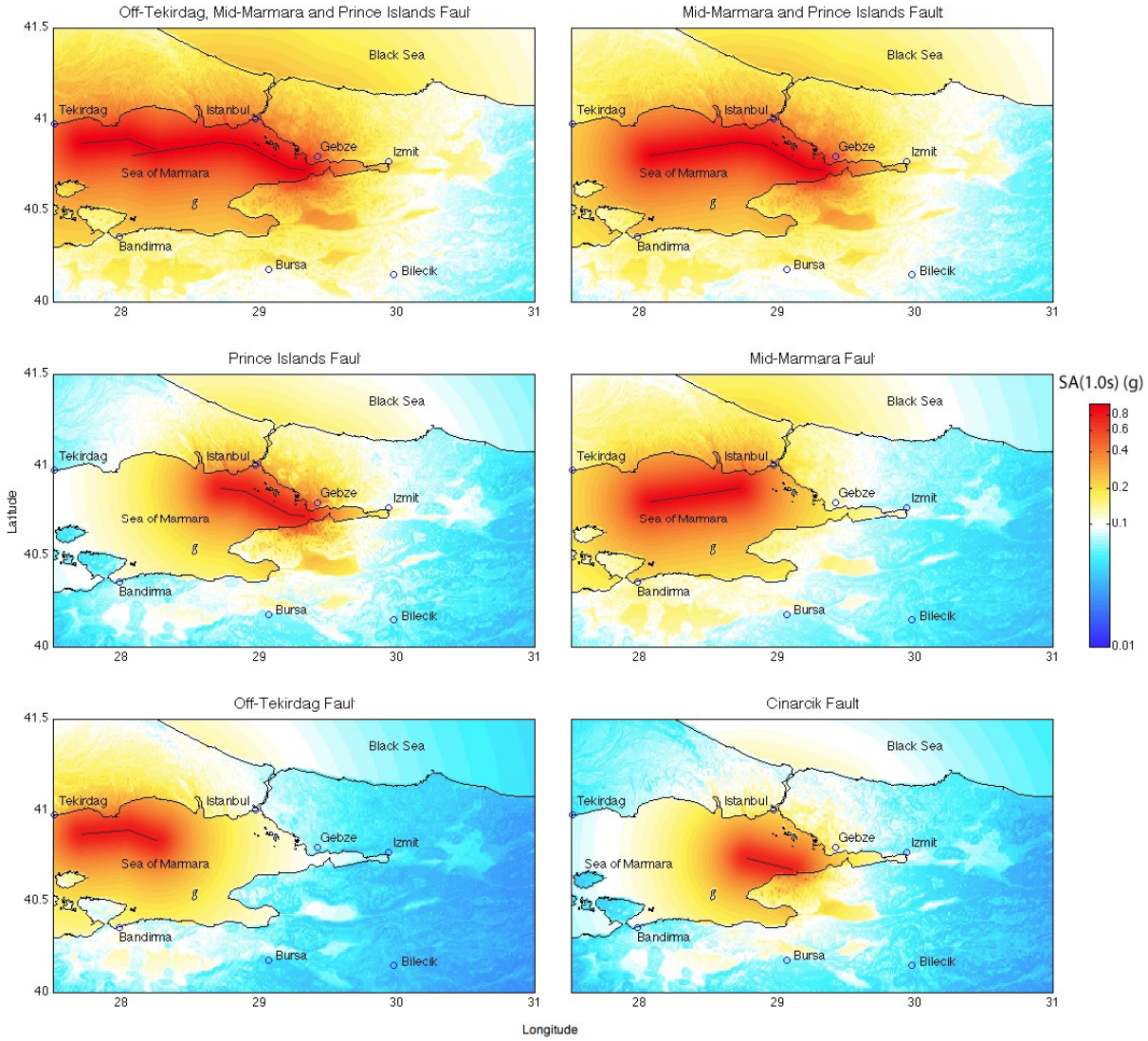

Figure 10. 5%-damped spectral acceleration (SA) at 1.0 sec estimates for the Sea of Marmara region considering six plausible earthquake scenarios.

In **Figure 11**, close-up views of the median values of PGA for the Istanbul metropolis are shown. The distribution of PGA values, shown by the color gradient, indicates a higher shaking level along the coastline of Istanbul, where Off-Tekirdağ, Mid-Marmara, and Islands faults are about 10–15 km offshore. Multiple rupturing of these fault segments is expected to shake the coastal districts of the city on the European side (these are Avcılar, Bahçeşehir, Bakırköy, and Beylikdüzü) with a PGA of 0.5–0.7 g. Intense PGA levels are also expected at the Istanbul Strait, where it opens to the Sea of Marmara. The level of shaking gradually diminishes toward the north. The median PGA ranges between 0.4 g and 0.6 g in the coastal districts of the city on the Asian side (these are Kadıkoy, Maltepe, Kartal, Pendik, and Tuzla). The estimated PGA increases to as much as 0.65 g in Adalar district (Marmara Islands).

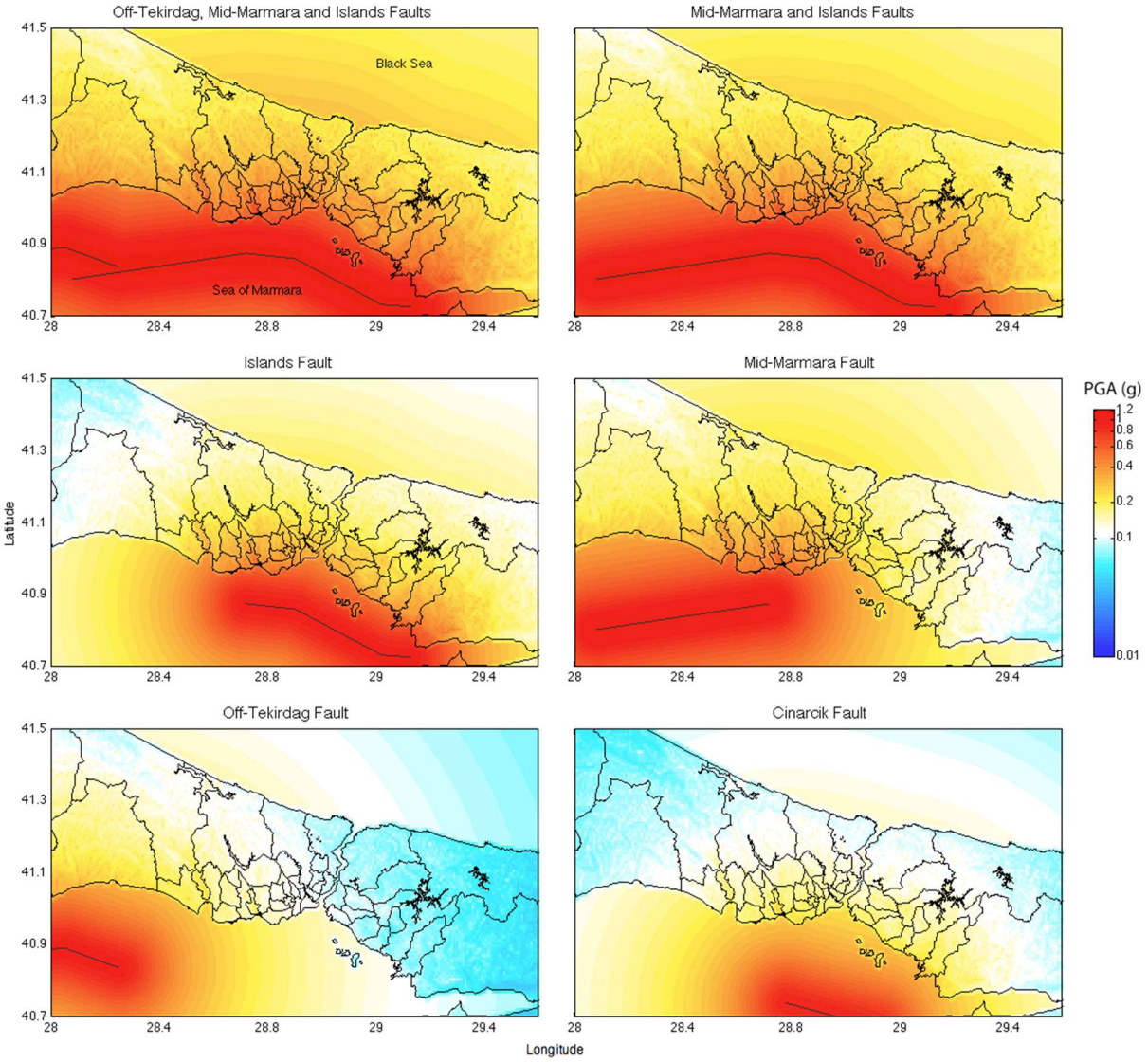

Figure 11. Close-up to peak ground acceleration (PGA) estimates for the Istanbul metropolitan area considering six earthquake scenarios. The median computed PGA is 0.65 g along the shoreline to the west of Istanbul (Bakırkoy district) and at Marmara Islands (Adalar discrict) as a result of multiple rupturing of Off-Tekirdağ, Mid-Marmara, and Islands faults; map (top panel) shows districts of the Istanbul Metropolitan Area.

Figure 12 shows the districts of the Istanbul metropolitan area, and **Table 1** lists the PGA and SA values at 0.2, 0.3, 0.5, 1, 1.5, 2, 3, and 4 s computed at the central point of each district considering the worst-case earthquake scenario (that is, multiple rupturing of Off-Tekirdağ, Mid-Marmara, and Islands fault segments). In this table, the districts expected to experience the highest shaking are also highlighted. This table shows that the largest expected spectral acceleration at short periods (0.3 s) that are close to the fundamental vibration period of 3- and 4-story reinforced concrete buildings is close to 1 g along the shoreline to the west of Istanbul and at the Sea of Marmara islands. The majority of the building stock in these parts of the city, including those at Avcılar, Bakirkoy, Bahçeşehir, and Adalar districts, are 3–5 story heights, which are the most vulnerable. At the city's financial district (Sarıyer), which has mostly mid- and high-rise buildings (5- to 30-story), the largest expected spectral acceleration at 0.5, 1, and 3 s are 0.24, 0.2, and 0.07 g, respectively. This level of shaking indicates that the financial district of the city will be shaken in much less intensity than its shoreline.

Table 1. Peak ground acceleration (PGA) and spectral acceleration (SA) values (at 0.2, 0.3, 0.5, 1, 1.5, 2, 3, and 4 s for 5%-damping) computed at central point of districts in the Istanbul metropolitan area considering the worst-case earthquake scenario (that is, multiple rupturing of Off-Tekirdağ, Mid-Marmara and Islands fault segments). The districts, expected to experience the highest shaking, are highlighted.

District name	Population	Area	Population density		Spectral accelerations (g)							
		(km^2)	(people/km^2)	PGA (g)	(0.2 s)	(0.3 s)	(0.5 s)	(1 s)	(1.5 s)	(2 s)	(3 s)	(4 s)
Adalar	10,460	11.05	947	0.65	0.91	0.95	0.71	0.59	0.37	0.28	0.20	0.15
Arnavutköy	148,419	506.5	293	0.27	0.36	0.37	0.27	0.24	0.16	0.12	0.09	0.07
Ataşehir	345,588	25.87	13,359	0.42	0.57	0.57	0.41	0.36	0.23	0.17	0.13	0.10
Avcılar	322,190	41.92	7686	0.55	0.77	0.78	0.57	0.48	0.29	0.22	0.16	0.12
Bağcılar	719,267	22.4	32,110	0.38	0.53	0.53	0.39	0.33	0.21	0.15	0.11	0.08
Bahçelievler	571,711	16.57	34,503	0.56	0.74	0.77	0.55	0.48	0.32	0.24	0.19	0.14
Bakırköy	214,821	29.65	7245	0.65	0.87	0.90	0.65	0.56	0.37	0.28	0.21	0.16
Başakşehir	193,750	104.5	1854	0.37	0.50	0.51	0.37	0.32	0.21	0.15	0.11	0.08
Bayrampaşa	272,196	9.5	28,652	0.41	0.56	0.56	0.41	0.36	0.23	0.17	0.13	0.10
Beşiktaş	191,513	18.04	10,616	0.34	0.47	0.48	0.35	0.30	0.20	0.15	0.11	0.08
Beykoz	241,833	310.4	779	0.23	0.32	0.32	0.24	0.21	0.13	0.10	0.07	0.05
Beylikdüzü	186,847	37.74	4951	0.52	0.72	0.73	0.53	0.45	0.28	0.20	0.15	0.11
Beyoğlu	247,256	8.96	27,596	0.49	0.68	0.69	0.50	0.42	0.26	0.19	0.14	0.10
Büyükçekmece	151,954	157.7	964	0.45	0.62	0.63	0.46	0.40	0.26	0.19	0.15	0.11
Çatalca	61,566	1040	59	0.25	0.35	0.35	0.26	0.22	0.14	0.10	0.07	0.05
Çekmeköy	135,603	148	916	0.23	0.31	0.30	0.22	0.19	0.12	0.09	0.06	0.05
Esenler	468,448	18.51	25,308	0.37	0.51	0.52	0.38	0.33	0.21	0.16	0.12	0.09
Esenyurt	335,316	43.12	7776	0.49	0.65	0.67	0.48	0.43	0.28	0.22	0.17	0.13
Eyüp	317,695	228.1	1393	0.26	0.35	0.35	0.26	0.22	0.15	0.11	0.08	0.06
Fatih	455,498	15.93	28,594	0.50	0.67	0.68	0.49	0.44	0.29	0.22	0.17	0.13
Gaziosmanpaşa	464,109	11.67	39,769	0.34	0.47	0.48	0.35	0.30	0.19	0.14	0.10	0.08
Güngören	318,545	7.17	44,427	0.50	0.68	0.69	0.50	0.44	0.29	0.22	0.17	0.13
Kadıköy	550,801	25.07	21,971	0.46	0.63	0.64	0.46	0.41	0.27	0.20	0.16	0.12
Kağıthane	418,229	14.83	28,202	0.31	0.44	0.44	0.32	0.27	0.17	0.12	0.09	0.06
Kartal	427,156	38.54	11,083	0.52	0.70	0.72	0.52	0.45	0.29	0.22	0.17	0.12
Küçükçekmece	662,566	37.25	17,787	0.46	0.65	0.65	0.47	0.40	0.25	0.18	0.13	0.10
Maltepe	415,117	53.06	7824	0.41	0.56	0.57	0.42	0.36	0.23	0.17	0.12	0.09
Pendik	520,486	180.2	2888	0.43	0.61	0.61	0.44	0.37	0.23	0.17	0.12	0.09

Table 1. (*Continued*).

District name	Population	Area	Population density		Spectral accelerations (g)							
		(km^2)	(people/km^2)	PGA (g)	(0.2 s)	(0.3 s)	(0.5 s)	(1 s)	(1.5 s)	(2 s)	(3 s)	(4 s)
Sancaktepe	223,755	61.87	3617	0.26	0.36	0.36	0.27	0.23	0.15	0.11	0.08	0.06
Sarıyer	276,407	151.3	1827	0.23	0.32	0.31	0.24	0.20	0.13	0.09	0.07	0.05
Silivri	118,304	869.5	136	0.31	0.43	0.43	0.32	0.27	0.17	0.12	0.09	0.07
Sultanbeyli	272,758	28.86	9451	0.33	0.46	0.46	0.34	0.29	0.18	0.13	0.10	0.07
Sultangazi	436,935	36.24	12,057	0.34	0.46	0.47	0.34	0.30	0.20	0.16	0.12	0.09
Şile	25,169	781.7	32	0.18	0.24	0.24	0.18	0.16	0.11	0.08	0.06	0.04
Şişli	314,684	34.98	8996	0.42	0.56	0.58	0.42	0.37	0.25	0.19	0.16	0.12
Tuzla	165,239	123.9	1334	0.57	0.78	0.80	0.58	0.50	0.31	0.24	0.18	0.13
Ümraniye	553,352	45.3	12,215	0.40	0.54	0.55	0.40	0.36	0.24	0.19	0.15	0.11
Üsküdar	529,550	35.34	14,984	0.34	0.48	0.48	0.35	0.30	0.19	0.14	0.10	0.07
Zeytinburnu	288,743	11.31	25,530	0.53	0.73	0.74	0.54	0.46	0.30	0.22	0.17	0.13

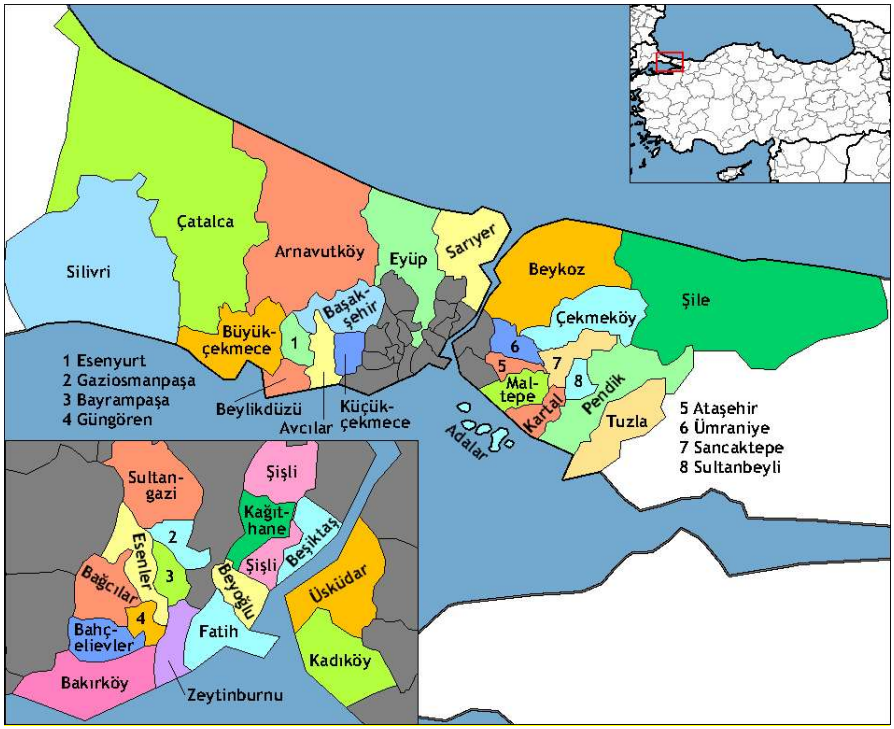

Figure 12. Districts of the Istanbul metropolitan area.

8. Comparing ground shaking with the 1999 M7.4 Kocaeli earthquake

Figure 13 showcases the comparative analysis where the Peak Ground Acceleration (PGA) ratio is calculated, contrasting the projected outcomes referenced in **Figure 11** with the actual PGA values recorded during the 1999 M7.4 Kocaeli earthquake in Istanbul. This analysis reveals that the western part of the Istanbul Metropolitan area could encounter ground-shaking intensities that exceed, by more than threefold, the levels experienced in the 1999 Kocaeli tremor.

9. Conclusions

In this study, we delved into the seismic hazards threatening Istanbul, a city on the cusp of a potential major earthquake. Our goal was to establish a robust scientific foundation for seismic design applications, evaluating the intensity of ground shaking across six well-defined earthquake scenarios. These plausible scenarios were constructed based on a rich blend of geological, tectonic, historical, and instrumental evidence, ensuring a comprehensive risk assessment.

We employed an objective approach in choosing logic-tree weights for Ground Motion Prediction Equations (GMPEs) and factored in the site-specific amplification effects of near-surface soils. This dual consideration allowed us to paint a more detailed picture of the seismic shaking hazards across the Sea of Marmara region.

The tangible outcome of our research is a set of deterministic seismic hazard maps that not only provide a granular view of potential risks but also serve to enhance the probabilistic seismic hazard maps introduced by Kalkan et al.[1]. These maps are primed for integration into the risk assessment and structural design processes within the Istanbul metropolitan area, serving as a crucial tool for both new constructions and the evaluation of existing structures. They underscore the need for improved design and construction methodologies aimed at mitigating loss of life and property in the face of seismic events.

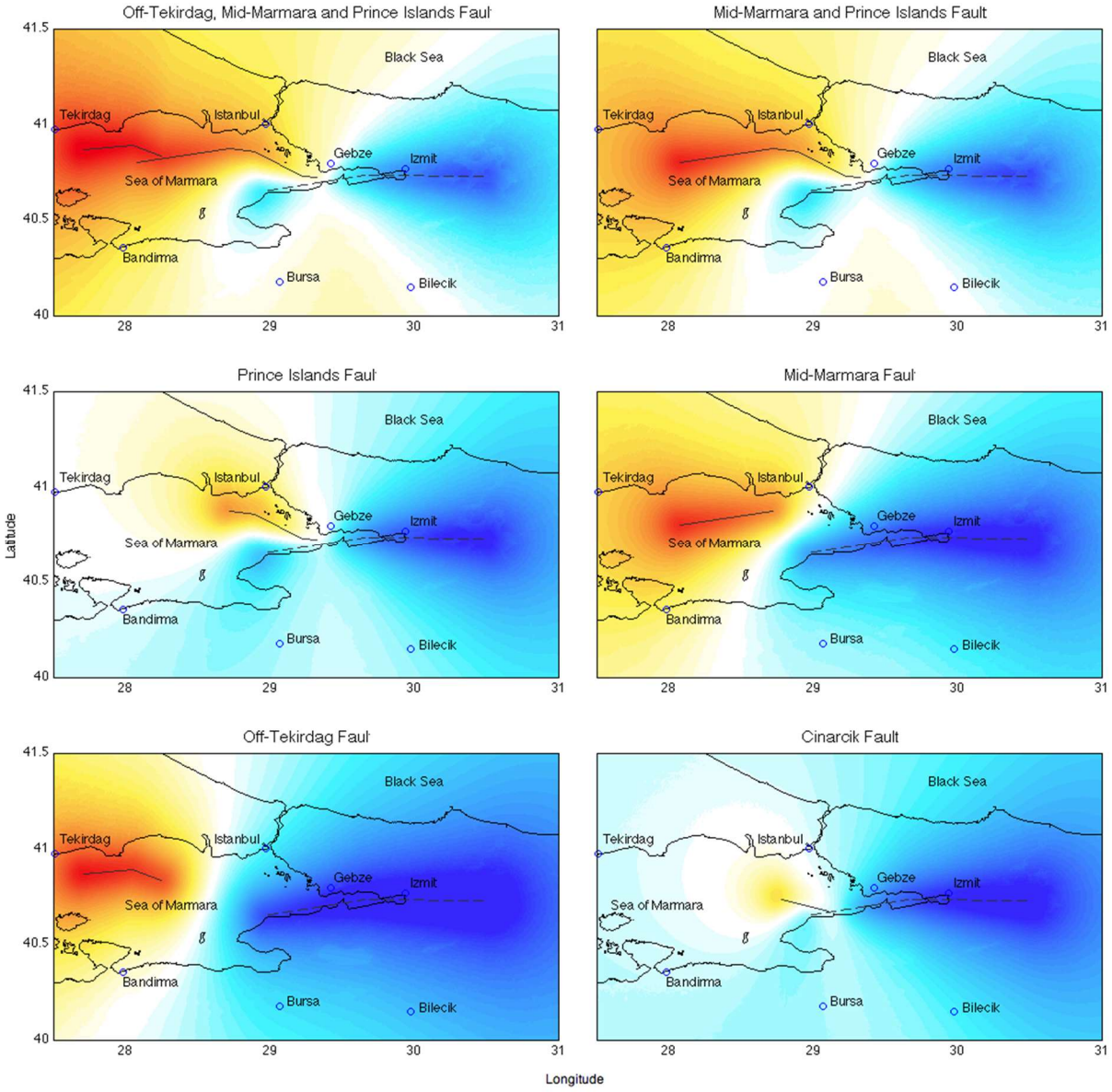

Figure 13. Ratio of PGA values of scenario earthquakes to the 1999 Kocaeli Earthquake shows that the west of the Istanbul Metropolitan area is expected to be shaken more than three times as it did during the Kocaeli Earthquake.

Moreover, our methodology has broader applications, extending to other seismically active regions such as eastern Turkey, which suffered from devastating earthquakes in 2023. Our findings offer a supplementary perspective to the Global Seismic Hazard Assessment Project, with our approach providing a more refined scale of analysis.

The study also addresses the potential integration of our methods into current design and construction regulatory frameworks, including the Turkish Seismic Design Code. This discussion underscores the practical implications of our findings and paves the way for their institutional implementation.

Lastly, we contemplate the strategic development of Istanbul, proposing rational zoning strategies informed by our seismic assessments. This element of the conclusion emphasizes the value of our research in supporting urban planning and the proactive mitigation of earthquake risks in Istanbul and similar urban environments.

Through these multifaceted conclusions, our study serves as a reminder of the power of informed, data-driven decision-making in enhancing structural resilience and public safety.

Author contributions

Conceptualization, EK and PK; methodology, EK and PK; software, EK; validation, EK and PK; formal analysis, EK and PK; investigation, EK and PK; resources, EK; data curation, EK; writing—original draft preparation, EK; writing—review and editing, EK and PK; visualization, EK; supervision, EK and PK; project administration, EK. All authors have read and agreed to the published version of the manuscript.

Acknowledgments

We extend our thanks to all contributors who played a pivotal role in the fruition of this paper. Special appreciation is due to Art Frankel for his essential guidance with the USGS deterministic seismic hazard code. We are thankful to Mahmut Baş for providing the district map of Istanbul province, and to Risk Management Solutions Inc., Newmark, CA, for their earthquake exposure plots that were crucial to our research. Our sincere gratitude is also directed to Ross Stein, Volkan Sevilgen, Charles Muller, Ayhan Irfanoglu, and Ömer Emre, whose meticulous reviews and insightful feedback have significantly elevated the technical rigor and clarity of this paper. Additionally, Margaret Segou's support with the DSHA computer codes and results was invaluable. We also acknowledge the USGS for supplying the data that enabled us to create the Vs30 proxy map, a vital component of our study.

Conflict of interest

The authors declare no conflict of interest.

References

1. Kalkan E, Gulkan P, Yilmaz N, et al. Reassessment of probabilistic seismic hazard in the Marmara Region. *Bulletin of the Seismological Society of America* 2009; 99(4): 2127–2146. doi: 10.1785/0120080285
2. Smith AD, Taymaz T, Oktay F, et al. High-resolution seismic profiling in the Sea of Marmara (northwest Turkey): Late Quaternary sedimentation and sea-level changes. *Geological Society of America Bulletin* 1995; 107(8): 923–936. doi: 10.1130/0016-7606(1995)107<0923: hrspit>2.3.co, 2
3. Parke, Minshull, Anderson, et al. Active faults in the Sea of Marmara, western Turkey, imaged by seismic reflection profiles. *Terra Nova* 1999; 11(5): 223–227. doi: 10.1046/j.1365-3121.1999.00248.x
4. Okay AI, Kaşlılar-Özcan A, İmren C, et al. Active faults and evolving strike-slip basins in the Marmara Sea, northwest Turkey: A multichannel seismic reflection study. *Tectonophysics* 2000; 321(2): 189–218. doi: 10.1016/s0040-1951(00)00046-9
5. Hubert-Ferrari A, Barka A, Jacques E, et al. Seismic hazard in the Marmara Sea region following the 17 August 1999 Izmit earthquake. *Nature* 2000; 404(6775): 269–273. doi: 10.1038/35005054
6. Parsons T, Toda S, Stein RS, et al. Heightened odds of large earthquakes near Istanbul: An interaction-based probability calculation. *Science* 2000; 288(5466): 661–665. doi: 10.1126/science.288.5466.661
7. Parsons T. Recalculated probability of M ≥ 7 earthquakes beneath the Sea of Marmara, Turkey. *Journal of Geophysical Research: Solid Earth* 2004; 109(B5). doi: 10.1029/2003jb002667
8. Kalkan E, Wills CJ, Branum DM. Seismic hazard mapping of California considering site effects. *Earthquake Spectra* 2010; 26(4): 1039–1055. doi: 10.1193/1.3478312
9. Wald DJ, Allen TI. Topographic slope as a proxy for seismic site conditions and amplification. *Bulletin of the Seismological Society of America* 2007; 97(5): 1379–1395. doi: 10.1785/0120060267
10. Wells DL, Coppersmith KJ. New empirical relationships among magnitude, rupture length, rupture width, rupture area, and surface displacement. *Bulletin of the Seismological Society of America* 1994; 84(4): 974–1002. doi: 10.1785/bssa0840040974
11. Armijo R, Meyer B, Navarro S, et al. Asymmetric slip partitioning in the Sea of Marmara pull-apart: A clue to propagation processes of the North Anatolian Fault? *Terra Nova* 2002; 14(2): 80–86. doi: 10.1046/j.1365-3121.2002.00397.x
12. Armijo R, Pondard N, Meyer B, et al. Submarine fault scarps in the Sea of Marmara pull-apart (North

Anatolian Fault): Implications for seismic hazard in Istanbul. *Geochemistry, Geophysics, Geosystems* 2005; 6(6). doi: 10.1029/2004gc000896
13. Le Pichon X, Şengör AMC, Demirbağ E, et al. The active Main Marmara Fault. *Earth and Planetary Science Letters* 2001; 192(4): 595–616. doi: 10.1016/s0012-821x(01)00449-6
14. Le Pichon X, Chamot-Rooke N, Rangin C, et al. The North Anatolian fault in the Sea of Marmara. *Journal of Geophysical Research: Solid Earth* 2003; 108(B4). doi: 10.1029/2002jb001862
15. Harris RA. The 1999 Izmit, Turkey, Earthquake: A 3D dynamic stress transfer model of intraearthquake triggering. *Bulletin of the Seismological Society of America* 2002; 92(1): 245–255. doi: 10.1785/0120000825
16. Pulido N, Ojeda A, Atakan K, et al. Strong ground motion estimation in the Sea of Marmara region (Turkey) based on a scenario earthquake. *Tectonophysics* 2004; 391(1–4): 357–374. doi: 10.1016/j.tecto.2004.07.023
17. Poliakov ANB, Dmowska R, Rice JR. Dynamic shear rupture interactions with fault bends and off-axis secondary faulting. *Journal of Geophysical Research: Solid Earth* 2002; 107(B11). doi: 10.1029/2001jb000572
18. Kame N, Rice JR, Dmowska R. Effects of prestress state and rupture velocity on dynamic fault branching. *Journal of Geophysical Research: Solid Earth* 2003; 108(B5). doi: 10.1029/2002jb002189
19. Abrahamson N, Silva W. Summary of the Abrahamson & Silva NGA ground-motion relations. *Earthquake Spectra* 2008; 24(1): 67–97. doi: 10.1193/1.2924360
20. Boore DM, Atkinson GM. Ground-motion prediction equations for the average horizontal component of PGA, PGV, and 5%-damped PSA at spectral periods between 0.01sand 10.0s. *Earthquake Spectra* 2008; 24(1): 99–138. doi: 10.1193/1.2830434
21. Campbell KW, Bozorgnia Y. NGA ground motion model for the geometric mean horizontal component of PGA, PGV, PGD and 5% damped linear elastic response spectra for periods ranging from 0.01 to 10s. *Earthquake Spectra* 2008; 24(1): 139–171. doi: 10.1193/1.2857546
22. Chiou BJ, Youngs RR. An NGA model for the average horizontal component of peak ground motion and response spectra. *Earthquake Spectra* 2008; 24(1): 173–215. doi: 10.1193/1.2894832
23. Stafford PJ, Strasser FO, Bommer JJ. An evaluation of the applicability of the NGA models to ground-motion prediction in the Euro-Mediterranean region. *Bulletin of Earthquake Engineering* 2007; 6(2): 149–177. doi: 10.1007/s10518-007-9053-2
24. Graizer V, Kalkan E. Ground motion attenuation model for peak horizontal acceleration from shallow crustal earthquakes. *Earthquake Spectra* 2007; 23(3): 585–613. doi: 10.1193/1.2755949
25. Graizer V, Kalkan E. Prediction of spectral acceleration response ordinates based on PGA attenuation. *Earthquake Spectra* 2009; 25(1): 39–69. doi: 10.1193/1.3043904
26. Akkar S, Aldemir A, Askan A, et al. 8 March 2010 Elazig-Kovancilar (Turkey) earthquake: Observations on ground motions and building damage. *Seismological Research Letters* 2011; 82(1): 42–58. doi: 10.1785/gssrl.82.1.42
27. Kalkan E, Gülkan P. Site-dependent spectra derived from ground motion records in Turkey. *Earthquake Spectra* 2004; 20(4): 1111–1138. doi: 10.1193/1.1812555